Check for updates

A low carbon balance triggers *Microvine* inflorescence abscission at high temperatures

Nathalie Luchaire[1,2†], Laurent Jean-Marie Torregrosa[1],
Yves Gibon[3,4], Markus Rienth[2†], Charles Romieu[2],
Agnès Ageorges[5], Olivier Turc[1], Bertrand Muller[1]
and Anne Pellegrino[1]*

[1]Laboratoire d'Ecophysiologie des Plantes sous Stress Environnementaux (LEPSE), Univ Montpellier,
Institut national de recherche pour l'agriculture, l'alimentation et l'environnement (INRAE), Institut
Agro, Montpellier, France, [2]Amélioration et Génétique de l'Adaptation des Plantes (AGAP), Univ
Montpellier, Institut national de recherche pour l'agriculture, l'alimentation et l'environnement
(INRAE), Institut Agro, Montpellier, France, [3]Biologie du Fruit et Pathologie (BFP), Institut national de
recherche pour l'agriculture, l'alimentation et l'environnement (INRAE), Univ. Bordeaux, Villenave
d'Ornon, France, [4]MetaboHUB, Institut national de recherche pour l'agriculture, l'alimentation et
l'environnement (INRAE), Univ. Bordeaux, Villenave d'Ornon, France, [5]Sciences pour l'OEnologie
(SPO), Univ Montpellier, Institut national de recherche pour l'agriculture, l'alimentation et
l'environnement (INRAE), Institut Agro, Montpellier, France

Introduction: Global warming is a major threat to yield sustainability in most crops, including grapevine. Whether or not grapevine fruitfulness is impaired by an imbalance between carbon supply and demand caused by high temperatures was investigated in the present study.

Methods: Five experiments were conducted on *Microvine*, a natural mutant of grapevine that is insensitive to gibberellins, presents with a dwarf stature, and has continuous flowering along the vegetative axes. The last property was used to infer temporal patterns of inflorescence development from their spatial distribution at harvest. Two sets of plants, characterized by low or high levels of initial shoot vigor, were grown under contrasting day and night temperatures: 22°C/12°C and 30°C/20°C.

Results and discussion: The rate of leaf development of the main shoot was stable, regardless of the initial vigor and temperature treatment. In contrast, the warm temperatures delayed the timing of flowering for low-vigor plants or the onset of ripening for high-vigor plants. Fruitfulness was impaired by high temperatures as a result of the abscission of young inflorescences (before the flowering stage). From a careful spatiotemporal analysis of cluster abscission, we concluded that inflorescence drop under elevated temperatures was triggered by the increase in plant carbon demand due to the oldest clusters starting to unload sugars. Elevated temperatures may have also lowered the carbohydrate supply in the zone of inflorescence abscission due to the higher leaf respiration while all organ growth demand was maintained. Interestingly, inflorescence abscission occurred earlier when whole-plant vigor was low and was followed by a recovery period, in spite of a lower non-structural sugar status than in high-vigor plants. Taken together, our

results suggest that inflorescence abscission is linked to the variations of the carbon pool induced by changes in temperature and not to its absolute value. Our study, therefore, provides new hypotheses about the impacts of warm temperatures on the regulation of temperature-induced reproductive failure in grapevine.

Introduction

Climate change is a major concern for agriculture. According to climatic models, an increase in the maximum temperature during the summer ranging, on average, from 2.7°C to 4.3°C is expected in southern Europe in the next 50 years (Cardell et al., 2019). Global warming may be associated with more frequent and intense heat waves (Perkins-Kirkpatrick and Lewis, 2020). Such massive fluctuations of temperatures in a short period of time will dramatically impact the yield of several annual and perennial crops, including grapevine (Lobell et al., 2006; Moriondo et al., 2011; Fraga et al., 2016).

Part of the negative effect of warming on crop yield may be attributed to the shift in the phenological cycle (Chmielewski and Rötzer, 2001; Yaacoubi et al., 2014). In grapevine, earlier budburst, flowering, onset of ripening (*véraison*), and ripening are observed worldwide as a consequence of warming (Van Leeuwen et al., 2019). This warming increases the likelihood of exposure of the key stages of flower and berry development to critical heat and to other abiotic hazards, such as frost and water deficits (Sgubin et al., 2018). Beyond their impact on phenology, warm temperatures accelerate plant organogenesis. Leaf development rate is assumed to linearly increase with temperature, within a temperature window specific to each plant species (*ca.* 10°C –30°C for grapevine), and then to decrease (Lebon E. et al., 2004; Parent et al., 2010). Outwith extreme temperatures, the phyllochron (i.e., the time between the appearance of two successive leaves) is rather stable (Lebon E. et al., 2004). Plant vegetative biomass accumulation is often promoted by warm temperatures in both annual and perennial species (Thomas et al., 2007; Suwa et al., 2010). However, the partitioning between and within organs changes a lot with temperature. Warm temperatures favor the fraction of biomass allocated to the leaves and stems at the expense of roots (Thomas et al., 2007; Poorter et al., 2012; Vasconcelos Ribeiro et al., 2012). In addition, elevated temperatures lower the leaf dry mass per unit area, indicating fewer cell layers and protein content per unit of leaf area (Poorter et al., 2009; Vile et al., 2012; Wang et al., 2012).

Elevated temperatures also differentially impact the partitioning of non-structural carbohydrates (NSCs) toward the reserve organs. The short-term reserves (i.e., those supporting night growth and showing day–night fluctuations) are located in vegetative organs, such as stems and leaves, whereas the long-term reserves accumulate preferentially in the roots and wood (in perennial crops) and in reproductive organs such as grains and fruits (in annual and perennial crops). Short-term reserves display strong homeostasis with regard to the prevailing environmental conditions, as changes in temperature or photoperiod are compensated by changes in synthesis and degradation rates (Gibon et al., 2004). In contrast, the emerging picture is that long-term storage toward the grain and fruits (Keeling et al., 1993; Adams et al., 2001), or to the trunk and/or roots (Rogiers et al., 2011; Sadras and Moran, 2013a), is decreased in warm temperatures.

The carbon reserve depletion as temperatures increase denotes an imbalance between the supply and demand. For most species, carbon gain through photosynthetic processes increases in the temperature range of 15°C–35°C and then decreases with enzyme inactivation (Allakhverdiev et al., 2008). Furthermore, warm temperature stimulates the carbon consumption for dark respiration and photorespiration (for C3 plants), thus lowering the net carbon gain, at least in the short term (Way and Sage, 2008). In the longer term, as photosynthesis and respiration exhibit a coupled acclimation response to temperature, the carbon loss in warm temperatures may be buffered (Dewar et al., 1999; Drake et al., 2019).

Sugars are essential for gametophyte development, fertilization, and the coordination of embryonic and surrounding tissue development (Ruan et al., 2012). In fact, sugars act as growth signals, regulate cell division, and provide carbon skeletons for growth. The elevation of day and night temperatures at flowering triggers flower and seed or fruit abscission in several annual and perennial species, thus reducing the final yield (Wheeler et al., 2000; Prasad et al., 2008). Although the cascade of physiological events underlying flower, seed, or fruit abortion under abiotic stress, such as elevated temperature, is complex, lower plant nutritional status appears to play a major role (Sawicki et al., 2015; Zhang et al., 2016; Sadok and Jagadish, 2020). However, in perennial crops such as grapevine, plant nutritional status at fruit set is critical, as it occurs specifically when the plant switches from heterotrophy to autotrophy and when the plant growth rate is at its maximum (Zapata et al., 2004a; Lebon et al., 2008). Finally, in the case of perennials, higher levels of carbon storage during the preceding season are important for countering the fruit respiratory demand as a result of the warm temperatures, which may be exacerbated under high crop load (Rogiers et al., 2011; Sadras and Moran, 2013a).

In the present study, we hypothesized that grapevine fruit abortion at high temperature is due to an altered carbon balance. *Microvine* is a natural gibberellic acid-insensitive mutant, which presents with dwarf stature and continuous flowering along the vegetative axes (Chaïb et al., 2010; Torregrosa et al., 2019). This plant model can be used to overcome the difficulties underlying experiments on grapevine conducted in controlled environments (i.e., large plant size and extended reproductive cycle). In addition, because of the similar temporal patterns of leaf and berry growth among several phytomers (i.e., fundamental structural units of the plant) along the main axis of *Microvine*, temporal growth patterns can be inferred from spatial developmental data, thus allowing original and accurate experimental designs (Luchaire et al., 2017). The experiments were performed on two sets of *Microvine*, displaying high or low initial vigor. The changes in the spatial profiles of development, biomass accumulation, and flower/fruit abscission with regard to plant phenology, carbon gain, and sugar storage were addressed at different day/night temperatures, keeping all other climatic parameters identical.

Materials and methods

Plant material and growing conditions

Five experiments were performed with a 2-year-old, own-rooted, potted *Microvine* in 2011 (experiments 1 and 2) and in 2013 (experiments 3–5) in growth chambers (Table 1). Six to ten plants per experiment were thinned to keep a unique proleptic axis per plant (i.e., the main shoot issued from the winter bud). The sylleptic shoots (i.e., secondary shoots growing from axillary meristems) were removed as soon as they appeared. The plants were initially grown (period up to T0) in similar reference control conditions in a greenhouse with day/night temperatures of 25°C/15°C; a vapor pressure deficit (VPD) of 1.28 kPa, and a daily photosynthetically active radiation (PAR) over a 14-hour photoperiod of 19.2 mol m^{-2} d^{-1}. After T0, the plants were transferred to growth chambers and subjected to contrasting temperatures until harvest (Tf). The temperature treatments lasted 2 months for experiment 1 and 1 month for experiments 2–5. The day/night temperatures were set to 22°C/12°C and 30/20°C, respectively, for

TABLE 1 Environmental growth conditions of *Microvine* for the experiments with high-vigor (experiments 1 and 2) and low-vigor (experiments 3–5) plants and the main plant phenotypic traits.

		High vigor		Low vigor		
Experiment		1	2	3	4	5
Year		2011	2011	2013	2013	2013
Targeted day/night temperatures (°C)		22/12	30/20	25/15	30/15	30/25
Average daily weather conditions	Maximum/minimum temperature (°C)	22.28/12.68	29.67/19.60	24.54/15.41	29.11/14.81	29.75/23.95
	Cumulated PAR (mol m^{-2} d^{-1})	19.0	19.0	19.5	19.0	19.0
	Maximum/minimum VPD (kPa)	1.12/0.28	1.30/0.40	1.22/0.33	1.37/0.40	1.25/0.68
Plant number		8	8	6	10	10
Budburst date		November 2010	November 2010	January 2013	December 2012	December 2012
Cumulated thermal time after budburst at T0 (°Cd)		1520	1520	1000	700	700
Experiment duration (days)		58	29	35	30	30
Experiment duration (°Cd)		390	390	430	306	397
Phytomere number at T0		58 a	58 a	36 b	30 c	30 c
Phytomere number at Tf		75 a	75 a	51 b	46 c	50 b
Total leaf area at T0 (cm²)		3200 a	3200 a	1200 b	1400 b	1400 b
Total leaf area at Tf (cm²)		3700 a	4030 a	2000 b	2500 c	3100 a
Internode diameter at T0 (50% flowering phytomere, mm)		5.7 a	5.5 a	3.3 b	3.9 ab	4 ab
Maximal reproductive phenological stage at T0		Lag phase	Lag phase	Mid-flo.	Mid-flo.	Mid-flo.
Maximal reproductive phenological stage at Tf		*Véraison*	*Véraison*	Lag phase	Lag phase	Lag phase
Number of phytomeres bearing inflorescences at T0		8 a	8 a	5 b	4 b	4 b
Number of phytomeres bearing inflorescences at Tf		18 a	14 ab	15 ab	12 b	15 ab
Ratio of reproductive to total phytomers (Tf–T0)		0.59 a	0.35 a	0.67 a	0.5 a	0.55 a

The temperature treatments were imposed in growth chambers from T0 to Tf, after an initial growth period (before T0) in the greenhouse. The plants were harvested at Tf.
The different letters represent significant differences at a p-value = 0.05.

experiments 1 and 2. For experiments 4–6, they were set to 25°C/15°C (i.e., control temperatures), 30°C/15°C, and 30°C/25°C, respectively. Other climatic variables were similar for all experiments in 2011 and 2013. The average daily VPD ranged from 0.7 kPa for experiment 1 to 0.96 kPa for experiment 4. The average daily PAR, which was integral over a 14-hour photoperiod, was 19.0 mol m^{-2} d^{-1} –19.5 mol m^{-2} d^{-1} for all experiments.

Plant vigor and development at the onset of temperature treatments

The experiments performed during the two seasons, that is, 2011 (experiments 1 and 2) and 2013 (experiments 3–5), were designated as high and low vigor, respectively. These two classes were based on the plant's initial shoot vigor and developmental pattern at T0, as characterized by their internode diameter (5.6 mm *vs.* 3.7 mm, on average; Table 1). The maximum total number of unfolded phytomers was 58 and 36 for high- and low-vigor experiments, respectively. The crop load was homogenized at T0 by removing clusters beyond the flowering stage for low-vigor plants and beyond ripening for high-vigor plants.

Development and growth measurements

The date of budburst (modified Eichhorn-Lorenz (E–L) stage 4; Coombe, 1995) was assessed based on bud observations, which were conducted twice a week on each plant (Table 1). Then, the number of unfolded phytomers was counted twice a week over the period T0 to Tf. A phytomer was considered unfolded when the two foliar lobes separated by the main vein were in the same phyllotaxic plane. The rate of phytomer emergence permits the determination of the phyllochron, i.e., the growing degree-days (GDD) separating the appearance of two successive leaves on a shoot (Wilhelm and McMaster, 1995). The phyllochron was calculated for each plant from these measurements, as described previously by Luchaire et al. (2017). In addition, the total plant leaf area was determined at T0 and Tf from the sum of individual leaf areas at each phytomer position (Table 1).

In *Vitis vinifera* L. (including *Microvine*), phytomers are sequentially arranged as P0–P1–P2, with P0 phytomer bearing no inflorescence. Thus, the presence of any cluster at each P1 and P2 phytomer position along the axis was recorded at T0 and Tf for all plants. The numbers of flower buds, of flowers and of green or colored berries per cluster were counted via non-destructive observation at T0 and from destructive observation at Tf. The phytomer ranks from the apex (RFA), where flowering (and the onset of berry coloration) occurred, were determined. Flowering and the onset of berry coloration were defined as 50% of open flowers (modified E.L. stage 23) and 5% of berries colored (modified E–L stage 35), respectively (Coombe, 1995). In grapevines, berry coloration is called *véraison*. The onset of *véraison* follows the beginning of sugar accumulation in berries (Coombe, 1995). The term *véraison* will thus be used thereafter to refer to the onset of berry coloration and ripening.

The organs' dry biomass was measured at Tf. For this purpose, leaf disks and internodes, inflorescence rachis, and berries were collected. Only the young fully expanded vegetative organs (RFA 13), the rachis at flowering (50%), and the berries at *véraison* (5%) were selected and weighted. The berries at *véraison* were sampled for only experiments 1 and 2, as this stage was not reached for experiments 3–5 (Table 1). The samples were frozen, ground in liquid nitrogen, and stored at -80°C for further biochemical analyses. Aliquots of the powder obtained were taken and oven-dried at 60°C for 5 days for dry weight measurements.

Net photosynthesis and respiration measurements

Leaf net photosynthesis and respiration were measured two times over the period T0 to Tf. The measurements were performed using a LI-COR portable photosynthesis system (LI-6400XT pro; LI-COR, Inc., Lincoln, NE, USA) for experiments 1 and 2 and a CIRAS-2 portable photosynthesis system (PP Systems, Amesbury, MA, USA) for experiments 3–5. The PAR was provided for both apparatuses by a light-emitting diode (LED) light source, set to 0 μmol m^{-2} s^{-1} during the night and to 560 μmol m^{-2} s^{-1} during the day. The temperature within the leaf chamber was set to be identical to the specific day/night temperatures of the growth chamber for each experiment. The CO_2 concentration was set to 380 parts per million (ppm), and the relative humidity was adjusted to a VPD close to 1 kPa. Net photosynthesis and respiration were measured 1–6 hours after, and 1–5 hours before, the lamps were switched on, respectively. The measurements were performed at three leaf rank positions from the apex: RFA 5, 10, and 25. The individual area was also measured at each position to calculate the photosynthesis and respiration rates per leaf.

Biochemical analyses

The frozen powders of the leaves, internodes, rachis, and berries were assayed for glucose, fructose, sucrose, and starch concentrations using enzymatic assays as described by Gibon et al. (2009). The total soluble sugar (TSS) concentration was calculated as the sum of glucose, fructose, and sucrose concentrations. The total NSC concentration was calculated as the sum of TSS and starch concentrations.

Conversion of phytomer number to time and calculations of inflorescence abscission rate

The GDD after phytomer emergence was estimated at Tf for each RFA and all plants. It was calculated from the product of RFA and phyllochron, as previously proposed by Luchaire et al. (2017), see Equation 1:

$$GDD \ after \ phytomer \ emergence \ (°Cd)$$

$$= \ RFA \ \times \ Phyllochron. \hspace{2cm} (1)$$

The plant inflorescence abscission rate was determined at Tf for each RFA by considering separately two zones (i.e., proximal *vs.* distal zones) on the proleptic axes. The proximal zone included the phytomers bearing inflorescences prior to the flowering stage at T0 ($P_{T0< \ flo}$). The distal zone included the phytomers differentiated after T0 (P_{new}). The inflorescence abscission rate (Abs.rate) for the proximal zone thus corresponded to the ratio of the inflorescence number at Tf to the inflorescence number T0 (see Equation 2). For the distal zone, the Abs.rate was calculated as the ratio of the inflorescence number at Tf to the potential inflorescence number deducted from the phytomer types (P0–P1–P2) in this zone (see Equation 3):

Proximal zone : $\hspace{4cm} (2)$

$$Abs. \ rate \ (\%) \ = \ \frac{Inflo. \, number \ \, (PT0 < flo)_{Tf}}{Inflo. \, number \ \, (PT0 < flo)_{T0}} \ \times \ P100$$

Distal zone :

$$Abs. \ rate \ (\%) \ = \ \frac{Inflo. \, number \ \, (Pnew)_{Tf}}{Potential. \, Inflo. \, number \ \, (Pnew)_{Tf}} \ \times \ P100$$

$$\hspace{10cm} (3)$$
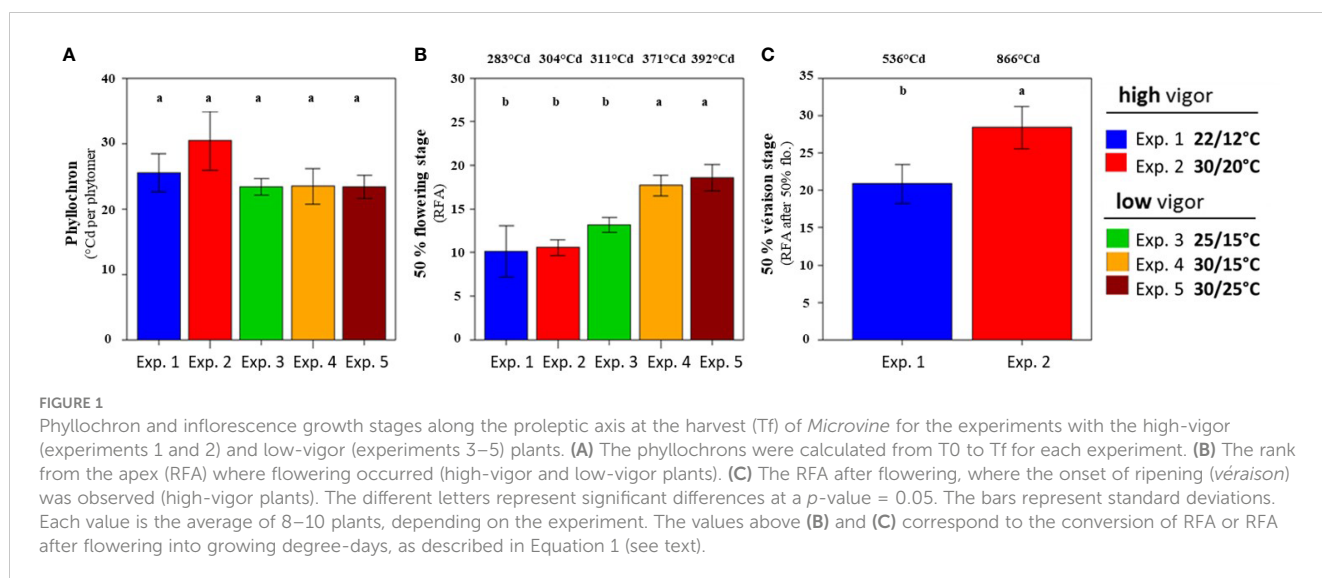
Statistical analyses

All statistical tests were conducted using R (R2.13.2; Foundation for Statistical Computing, Vienna, Austria). The Shapiro–Wilk test of normality was used first to analyze the distribution of the data set. Then, a one-way ANOVA, with either the least significant difference (LSD) multiple-comparison method (when data were normal) or Wilcoxon signed-rank tests (when normality could not be established), was performed for comparisons of the means. Because of the variation of the temperature treatments among the high- and low-vigor plants, the combination "vigor × temperature", rather than the individual effects of vigor and temperature were considered for mean comparisons.

Results

Phyllochron was stable at elevated temperatures, but flowering and the onset of ripening were delayed

The rate of vegetative development (as measured by the time between the emergence of two successive leaves, i.e., the phyllochron) of the *Microvine* was stable (Figure 1A). It reached around 25°Cd, irrespective of the temperature treatments (22°C/12°C to 30°C/25°C) and initial plant vigor (high *vs.* low vigor). This stability of the phyllochron allowed the comparison of the temporal patterns of inflorescence development between experiments from their spatial distribution along the axis. The timings of flowering and of the onset of ripening (or *véraison*; i.e., 5% of colored berries) were thus addressed at harvest (Tf), based on their ranks counted from the apex (RFA) or from the GDD after the phytomer emergence (i.e., the product of the RFA and the phyllochron). Flowering occurred between RFA 10 and 18 (i.e., 283°Cd and 392°Cd after phytomer emergence), depending on the temperature treatments and initial plant vigor (Figure 1B). When the initial vigor was low, elevated temperatures delayed flowering. Furthermore, flowering shifted from RFA 13 for the control (25°C/15°C, experiment 3) up to RFA 18 under high temperatures (30°C/15°C and 30°C/25°C, experiments 4 and 5, respectively). By contrast, flowering occurred at similar RFA (10 or 11) for high-vigor experiments, regardless of the temperature treatments (22°C/12°C and 30°C/20°C, experiments 1 and 2, respectively). *Véraison* was only observed in experiments 1 and 2, as experiments 3–5 were not designed to reach this stage (Table 1). Elevated temperatures delayed *véraison* (Figure 1C). Furthermore, *véraison* occurred on RFA after flowering 20 and 28 (i.e., 536°Cd and 866°Cd after the phytomer

FIGURE 1
Phyllochron and inflorescence growth stages along the proleptic axis at the harvest (Tf) of *Microvine* for the experiments with the high-vigor (experiments 1 and 2) and low-vigor (experiments 3–5) plants. **(A)** The phyllochrons were calculated from T0 to Tf for each experiment. **(B)** The rank from the apex (RFA) where flowering occurred (high-vigor and low-vigor plants). **(C)** The RFA after flowering, where the onset of ripening (*véraison*) was observed (high-vigor plants). The different letters represent significant differences at a *p*-value = 0.05. The bars represent standard deviations. Each value is the average of 8–10 plants, depending on the experiment. The values above **(B)** and **(C)** correspond to the conversion of RFA or RFA after flowering into growing degree-days, as described in Equation 1 (see text).

emergence) at cool (experiment 1) and high temperatures (experiment *2*), respectively.

In conclusion, while elevated temperatures had no impact on the phyllochron, they delayed reproductive development, either through delayed flowering under low vigor or through delayed *véraison* under high vigor, but apparently not both.

Fruitfulness was lower at elevated temperatures due to inflorescence abscission

Coulure, defined by flower and berry abscissions, was almost never observed in any of the experiments with *Microvine* in contrast to what can be observed in non-dwarf grapevine genotypes. *Coulure* was estimated at 1% during experiment 4 using a net attached to bunches and was thus considered negligible. By contrast, whole inflorescence abscissions were frequently observed (Figure 2A). Elevated temperatures tended to favor inflorescence drop (Figure 2B). The rate of inflorescence abscission calculated between RFA 3 at Tf and flowering at T0 ranged from 2% to 7% under cool and control temperatures (experiments 1 and 3, respectively). It increased under elevated temperatures from 11% (30°C/25°C, experiment 5) to 27% (30°C/20°C, experiment 2). As there was no compensation through flower or berry numbers on the remaining inflorescences (data not shown), up to one-quarter of the potential yield was lost during experiment 2. However, the ratio of reproductive phytomers to

the total number of phytomers did not differ among the temperature treatments, regardless of the initial vigor (Table 1).

The comparison of spatial patterns at harvest (Tf) and before the temperature treatment (T0) indicated that inflorescence abscission occurred at different times after the temperature treatment. The inflorescence decreased sooner (higher RFA) with a low initial vigor than with a high initial vigor (Figures 2A, B). Inflorescence abscission occurred from RFA 15 to RFA 35 for low-vigor plants (experiments 4 and 5). For high-vigor plants (experiment 2), it occurred from RFA 3 to RFA 20. In addition, the sensitivity to abscission was high for young inflorescences (prior to flowering time, defined as 50% of open flowers), although it was insignificant for more advanced inflorescences. Indeed, no inflorescence drop was observed in the zone of the axis below the flowering stage at T0 (Figure 2B).

Inflorescence abscission at elevated temperatures was concomitant with the onset of ripening

Whether or not the onset of ripening (*véraison*) could trigger inflorescence abscission was addressed for high-vigor plants (experiment 1, 22°C/12°C; and experiment 1, 30°C/20°C). For this purpose, the timings of inflorescence development (flowering and onset of ripening or *véraison*) over the temperature treatments were estimated from their spatial distribution (RFA) at T0 and Tf (Figure 3). For the purpose of estimation, the shift in
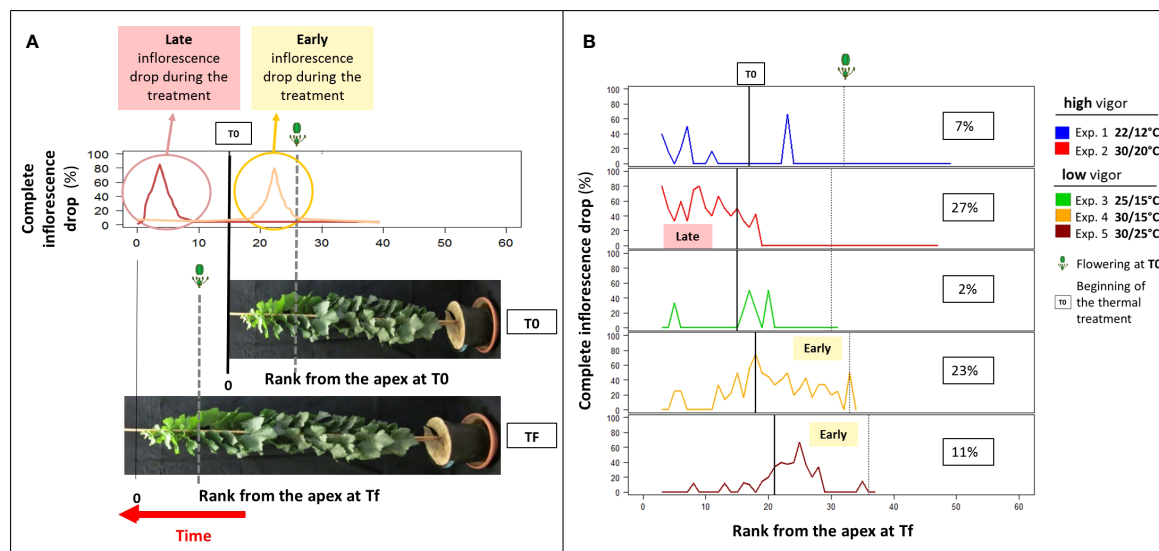

FIGURE 2
Microvine inflorescence abscission profiles along the proleptic axis at harvest (Tf). **(A)** The theoretical inflorescence abscission profiles and **(B)** the inflorescence abscission profiles for experiments with the high-vigor (experiments 1 and 2) and low-vigor (experiments 3−5) plants. **(A)** The theoretical inflorescence abscission profiles along the axis (rank from the apex, RFA) at Tf are schematized for two situations of late and early abscissions. The T0 vertical solid line delimits the phytomers that were unfolded before the temperature treatment (right) and the ones that were unfolded during the temperature treatment (left). The flowering stage at T0 and Tf is represented by the vertical dotted lines. The inflorescence abscission was limited to the zone of the axis above the flowering stage at T0. The rate of inflorescence abscission was calculated, as described in Equations 2 and 3 (see text), from the ratio between the inflorescence patterns at Tf and the inflorescence patterns at T0 (phytomers that were unfolded before T0) or a potential inflorescence pattern based on the phytomer types (P0−P1−P2) (phytomers that were unfolded after T0). **(B)** The inflorescence abscission profiles along the axis (RFA) at Tf for experiments 1−5 were drawn using the method explained in **(A)**. The vertical solid line and the vertical dotted line delimit the number of phytomers that were unfolded at T0 and the flowering stage at T0, respectively. The inflorescence abscission rates are the average of 8−10 plants, depending on the experiment.
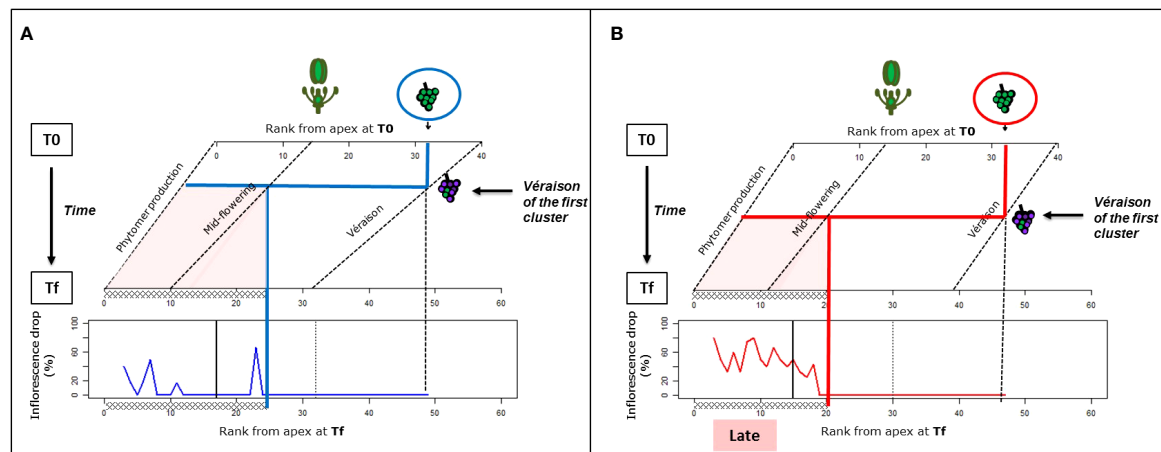
FIGURE 3
Impact of the onset of *véraison* on the inflorescence abscission in *Microvine* for the experiments with the high-vigor plants at cool temperatures [**(A)**, experiment 1] or elevated temperatures [**(B)**, experiment 2]. The rank from the apex (RFA), where flowering and the onset of ripening (*véraison*) occurred during the period from T0 to Tf, and the resulting possible zone of inflorescence drop (red-colored zone), were estimated. This sensitive zone for inflorescence drop was thus superimposed on to the inflorescence abscission profiles at Tf, originating from Figure 2B. The RFA where flowering at T0 and Tf and the onset of *véraison* at Tf occurred were derived from Figure 1. The onset of *véraison* at T0 was set on RFA 40, based on the observations of an independent batch of plants grown in similar conditions. The flowering and *véraison* progression along the axis from T0 to Tf were assumed to be linear. The oblique dotted lines represent the evolutions of phytomer production, flowering, and *véraison* RFA over this period. The vertical dotted line represents the RFA where *véraison* started on the first cluster, and the black vertical solid line delimits the phytomers that were unfolded before the temperature treatment (T0). The thick blue and red lines outline the onset of *véraison* on the first cluster, and the sensitive zone for inflorescence drops along the axis, including the phytomers above the flowering stage at *véraison*.

inflorescence development over this period was assumed to be linear. At T0, as all proximal inflorescences that had passed the lag phase were removed, the timing of *véraison* (corresponding to RFA 40) was determined from the observations on an independent set of high-vigor plants that were grown under similar conditions.

The developmental framework obtained for experiments 1 and 2 was then superimposed with the spatial pattern of inflorescence abscission at Tf (Figure 2) to delimit a sensitive temporal area for inflorescence abscission. This area was bounded by (i) the inflorescence abscission RFA zone at Tf (i.e., RFA 3–20 for experiment 2 and up to RFA 25 for experiment 1) and (ii) the timing of flowering of the most proximal inflorescence of this zone, as no abortion occurred after flowering. Defined as such, the onset of abortion was concomitant with the timing of *véraison* of the first cluster on the axis.
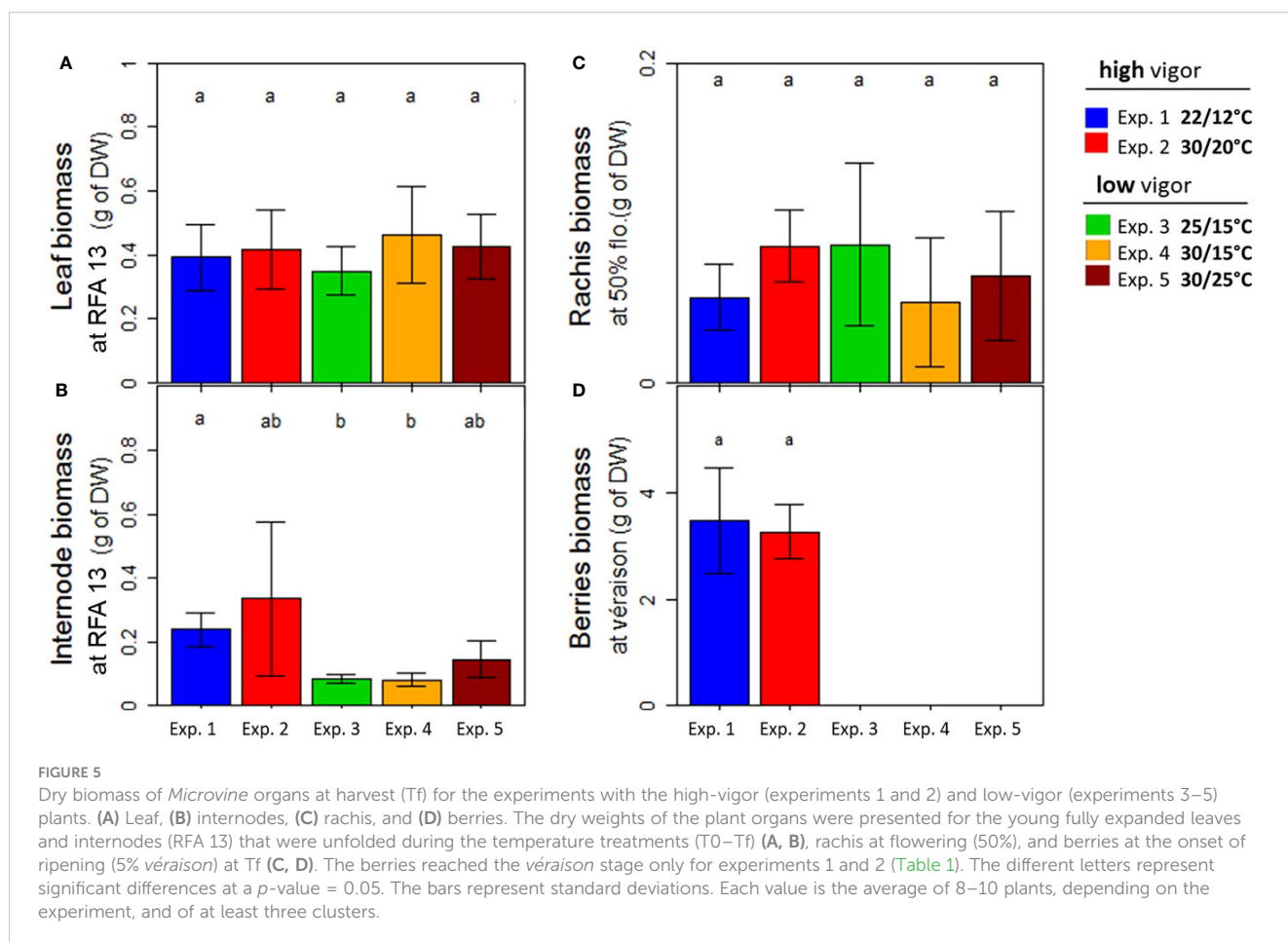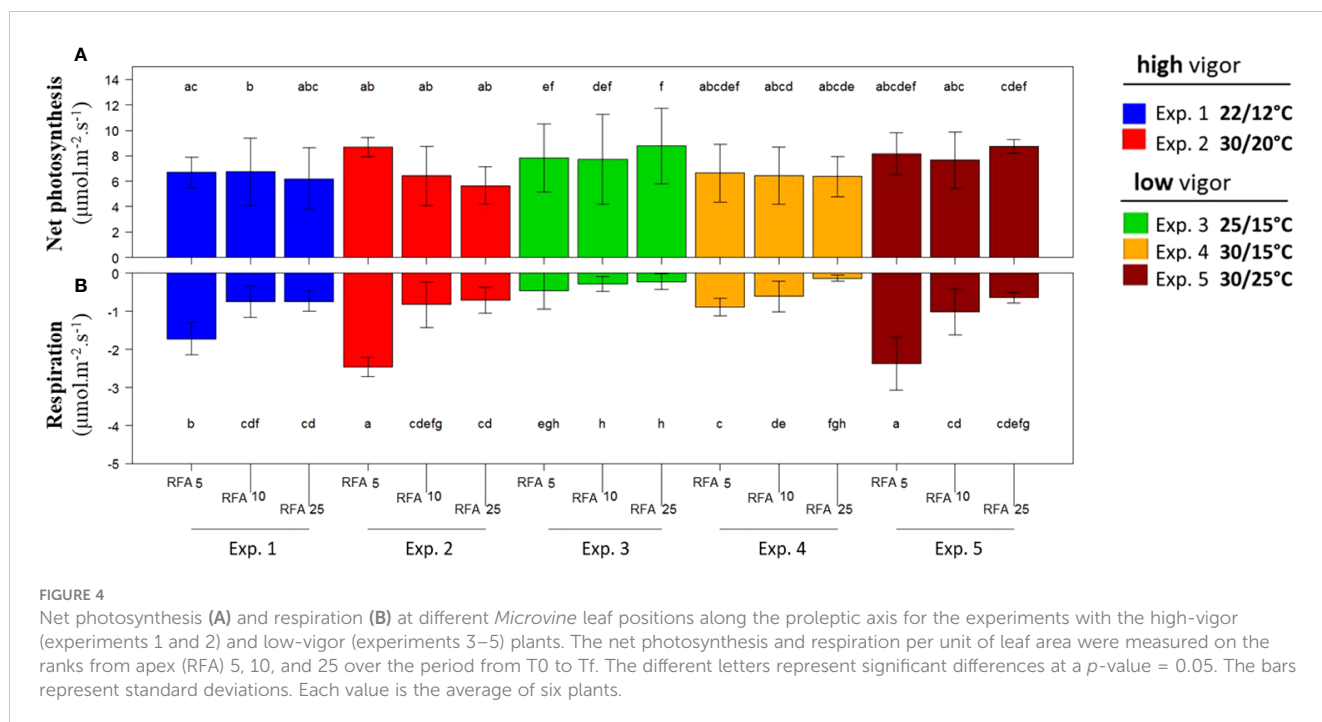
Thus, inflorescence abscission under elevated temperatures (experiment 2) and to a lesser extent under cool temperatures (experiment 1), could clearly be linked to the onset ripening of the oldest clusters for high-vigor experiments.

Elevated temperatures lowered carbohydrate supply while maintaining growth demand

Net photosynthesis and respiration per unit of leaf area were measured on RFA 5, RFA 10, and RFA 25 during the temperature treatments (T0 to Tf) for high-vigor and low-vigor plants (Figure 4). Net photosynthesis was stable, regardless of the leaf rank, the temperature treatment, and the initial plant vigor (Figure 4A). It ranged from 6 µmol m^{-2} s^{-1} to 9 µmol m^{-2} s^{-1}. In contrast, the

respiration was higher for RFA 5 than for RFA 10 and RFA 25, and it was also higher at elevated temperatures for RFA 5 and RFA 10 (experiments 2, 4, and 5) than in the cool or control temperature treatments (experiments 1 and 3, respectively) (Figure 5B). Thus, the respiration varied from –0.2 µmol m^{-2} s^{-1} to –2.2 µmol m^{-2} s^{-1}, depending on leaf age and temperature. As similar results were obtained when considering the net photosynthesis and respiration per leaf (Figure S1), the net carbon supply under elevated temperatures was lower in the zone of the axis prone to inflorescence abscission (i.e., RFA 15–35 and RFA 3–25 for plants with low and high initial vigor, respectively, as shown in Figure 2B).

The demand of newly formed organs between the temperature treatment periods was then analyzed based on their dry weights at Tf (Figure 5). For this purpose, young, fully expanded vegetative organs (leaves and internodes) at RFA 13 were selected. This zone was extended for inflorescences in order to include rachis at flowering (50%) and berries at the onset of ripening (5% *véraison*). The warmest experiments (experiments 2, 4, and 5) did not change the leaf dry weight, which was also similar between the two initial vigor conditions (Figure 5A). A tendency toward heavier internodes with elevated temperatures was detected (Figure 5B). However, the most striking difference was found between the 2 years and with the different initial vigors. In fact, the newly formed internodes were two- to threefold heavier for plants with a high level of initial vigor (experiments 1 and 2) than for plants with a low initial vigor (experiments 3–5). Similarly to the leaves, the rachis dry biomass was little impacted by the temperature treatment and initial vigor (Figure 5C). As already mentioned, *véraison* occurred later under warm temperatures (experiment 2) than under control temperatures (*experiment 1*).

FIGURE 4
Net photosynthesis **(A)** and respiration **(B)** at different *Microvine* leaf positions along the proleptic axis for the experiments with the high-vigor (experiments 1 and 2) and low-vigor (experiments 3–5) plants. The net photosynthesis and respiration per unit of leaf area were measured on the ranks from apex (RFA) 5, 10, and 25 over the period from T0 to Tf. The different letters represent significant differences at a *p*-value = 0.05. The bars represent standard deviations. Each value is the average of six plants.

FIGURE 5
Dry biomass of *Microvine* organs at harvest (Tf) for the experiments with the high-vigor (experiments 1 and 2) and low-vigor (experiments 3–5) plants. **(A)** Leaf, **(B)** internodes, **(C)** rachis, and **(D)** berries. The dry weights of the plant organs were presented for the young fully expanded leaves and internodes (RFA 13) that were unfolded during the temperature treatments (T0–Tf) **(A, B)**, rachis at flowering (50%), and berries at the onset of ripening (5% *véraison*) at Tf **(C, D)**. The berries reached the *véraison* stage only for experiments 1 and 2 (Table 1). The different letters represent significant differences at a *p*-value = 0.05. The bars represent standard deviations. Each value is the average of 8–10 plants, depending on the experiment, and of at least three clusters.

However, berry biomass at *véraison* was similar for experiments 1 and 2 (Figure 5D).

To conclude, elevated temperatures lowered the carbohydrate supply in the zone of inflorescence abscission due to a higher leaf respiration rate while maintaining all-organ growth demand. The non-respiratory organs' demand was similar regardless of the initial vigor, except for the internodes, which were higher for the high-vigor plants.

The effects of elevated temperatures on non-structural sugar accumulation in vegetative and reproductive organs at harvest highly relied on the initial plant vigor.

Total NSC concentrations in the vegetative (leaf and internode) and reproductive (rachis and berries) organs were determined at harvest for experiments 1–5. The same stages as for dry biomass assessment were selected, corresponding to the young fully expanded vegetative organs (RFA 13), rachis at flowering (50%), and berries at the onset of ripening (5% *véraison*).

The first picture emerging from these data was the difference in the NSC concentrations between the plants with high (experiments 1 and 2) and low (experiments 3–5) initial vigor (Figure 6). The leaf NSC concentration reached 75 mg g^{-1} in cool temperatures (experiment *1*) and up to 100 mg g^{-1} in warm temperatures (experiment 2) for the high-vigor plants (Figure 6A). In contrast, it did not exceed 35 mg g^{-1}, regardless of the temperature treatment for the low-vigor plants (experiments 3–5). The NSC concentration in the internodes was the highest for the low-temperature treatment of high-vigor plants (experiment 1), reaching 48 mg g^{-1} (Figure 6B).

For other experiments (experiments 2–5), similar NSC concentrations in the internodes (19 mg g^{-1}, on average) were observed. The rachis at flowering reached similar NSC concentrations (32 mg g^{-1}, on average) for all situations of vigor and temperature treatments (Figure 6C). Ultimately, the NSC concentrations in berries at *véraison* were only measured for high-vigor plants (experiments 1 and 2), and it was 43 mg g^{-1}, on average, for the two temperature treatments (Figure 6D).

To summarize, the total NSC concentration in the leaf and internode highly relied on the combined effects of initial vigor and temperature. High vigor favored the accumulation of NSC in leaves, regardless of temperature treatments, whereas warm temperatures decreased NSC accumulation in the internodes of plants with high initial vigor. Conversely, NSC concentrations was similar in rachis and berries, regardless of the vigor and/or temperature treatment.

Discussion

Reproductive development, but not vegetative development, is negatively impacted by elevated temperatures

The *Microvine* phyllochron was stable irrespective of temperature treatments (from +2.5°C to 8°C). It reached about 25°Cd (Figure 1A), similar to that observed for non-dwarf
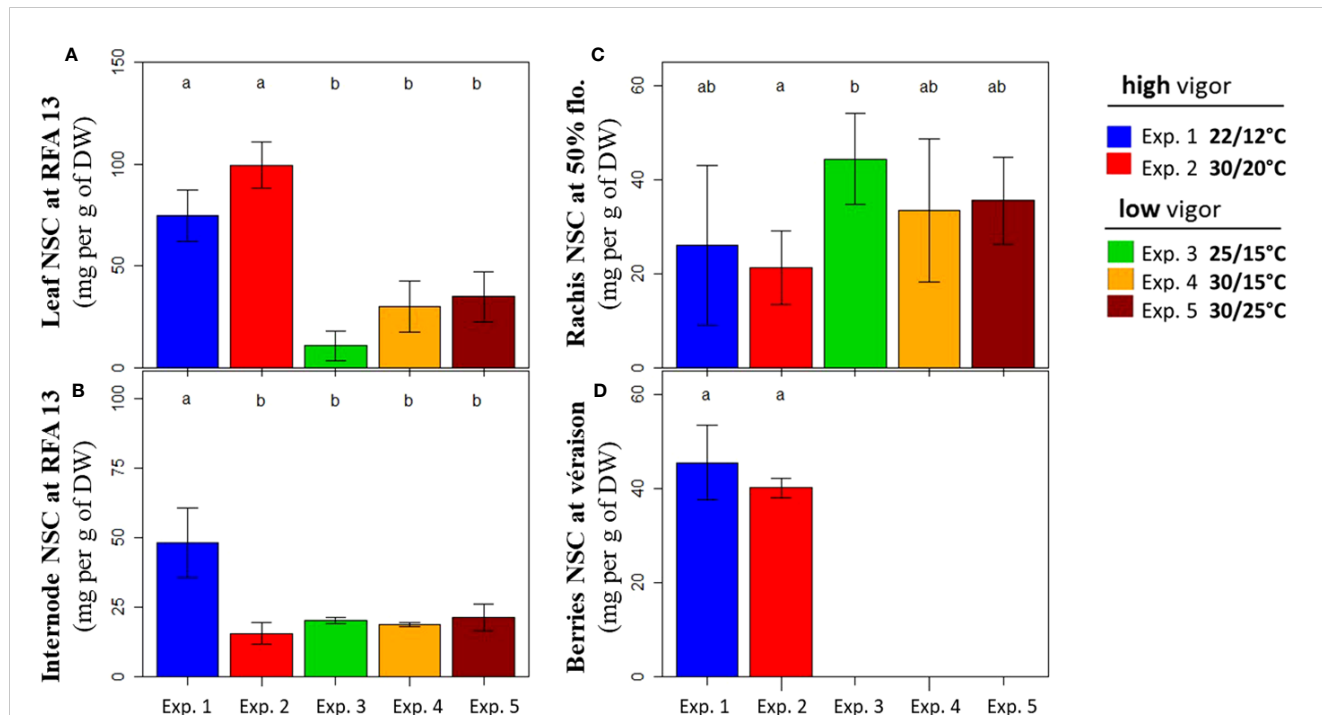

FIGURE 6
Non-structural carbohydrate (NSC) concentrations of *Microvine* organs at harvest (Tf) for the experiments with the high-vigor (experiments 1 and 2) and low-vigor (experiments 3–5) plants. **(A)** Leaf, **(B)** internodes, **(C)** rachis, and **(D)** berries. The NSCs of organs included glucose, fructose, sucrose, and starch (see text). The NSC concentrations were presented for the young fully expanded leaves and internodes (RFA 13) that were unfolded during the temperature treatments (T0−Tf) **(A, B)**, rachis at flowering (50%), and berries at the onset of ripening (5% *véraison*) at Tf **(C, D)**. The different letters represent significant differences at a *p*-value = 0.05. The bars represent standard deviations. Each value is the average of at least three plants.

grapevine genotypes (Lebon et al., 2004). The stability of the phyllochron has been extensively used for 60 years to standardize the developmental stages of growing plants (Meicenheimer, 2014), and *Microvine* makes no exception to this rule, whatever the temperature treatment. The leaf biomass was not impacted by the temperature treatments. In contrast, internode biomass slightly increased when warmer conditions (i.e., from +7.5°C to 8°C) were imposed (Figures 5A, B). Internode biomass increments can result from higher size and/or density. Previous studies on *Microvine* showed that elevated temperatures had little impact on the density of internodes but increased the specific leaf area (Luchaire et al., 2017). Thus, stable leaf biomass was likely to be associated with larger but thinner leaves, as reported for other species (Poorter et al., 2009; Wang et al., 2012). A possible reason for such a response could be the differential sensitivity of development and photosynthesis to elevated temperatures, the former being less sensitive than the latter (Parent et al., 2010; Hilty et al., 2021). Yet, in the present study, photosynthesis was hardly increased by daytime temperatures, which is in line with the hypothesis of a rapid acclimation to temperature (Yamori et al., 2014), whereas leaf respiration was stimulated (Figures 4A, B). We thus propose the hypothesis that the lower C supply-to-demand ratio has led to a "dilution" effect of dry matter into an increased leaf surface.

In contrast to vegetative development, reproductive development was delayed by temperature (Figures 1B, C). Flowering occurred later under warm temperatures (from +2.5°C to 7.5°C) when expressed in RFA (+5 ranks) and in thermal time (+81°Cd), but for low-initial-vigor plants only. Thus, elevated temperatures can delay flowering only when the initial reserve status is expected to be less favorable (Eltom et al., 2013). In accordance with those results, sugar supply and signaling were reported to be critical for the induction of flowering in both annual and perennial crops (Rolland et al., 2006; Sperling et al., 2019). The onset of ripening (5% *véraison*) was also delayed on an +8°C temperature treatment by as much as eight ranks; or 330°Cd. Such a delay in reproductive development under elevated temperature has already been reported for other fruit species (Civello et al., 1997; Adams et al., 2001; Torregrosa et al., 2017). In grapevine, the thermal effect on the onset of berry ripening was shown to be enhanced when the source-to-sink ratio was lower (Sadras and Moran, 2013b). Although the source-to-sink ratio of about 1 m²/kg for both high- and low-vigor plants may be considered balanced (Kliewer and Dokoozlian, 2005), the high decrease in sugar allocation to the internodes (Figure 6B) for plants with a high initial vigor under elevated temperatures was consistent with an alteration of carbon availability. Ultimately, those results suggest that the modulation of flowering and ripening processes by the interplay between resource-driven growth and temperature-driven development should be considered in the phenology model (Sperling et al., 2019).

In spite of the variations in the onset of ripening (5% *véraison*) and carbon functioning for high-vigor plants, the biomass and sugar allocations to the rachis at flowering and to the berries at *véraison* were unaffected by elevated temperatures (Figures 5C, D, 6C, D). This suggests that inflorescences follow a stable developmental program, independent of carbohydrate supply. In fact, the rate and duration of berry ripening, both at the levels of the individual berry and the population of berries, were shown to be more stable than the onset of ripening with respect to climatic variables, including temperature (Sadras and Petrie, 2011; Shahood et al., 2020). This observation fits with the distinction between developmental processes following mostly thermal rules (possibly modulated by carbon status) and those suspected to follow source limitation rules depending on the carbon provision through either reserve mobilization or light interception (which is the case of rapid sugar accumulation during ripening).

Inflorescence abscission under elevated temperatures presented two different patterns, depending on the initial plant vigor

The *coulure*, a term generally used to characterize flower and fruit abscission in grapevine (Dry et al., 2010), was not observed in *Microvine*, where fruit set is approximately 99% (data not shown). However, as we have previously reported (Torregrosa et al., 2019), whole inflorescence abscission was observed in *Microvine*. Complete inflorescence abortion has also been reported in hazel and cotton plants (Zhao et al., 2005; Liu et al., 2014). The rate of inflorescence abscission reached up to 27% under elevated temperatures (Figure 2B). Nevertheless, these yield losses are far from the ones observed in grapevine, where fruit abscission in optimal conditions normally ranges from 20% to 50% depending on the cultivar (Shavrukov et al., 2003; Lebon G. et al., 2004) and can reach up to 100% under adverse conditions (Greer and Weston, 2010).

The comparison of spatial patterns at harvest (Tf) and before temperature treatments (T0) indicated that inflorescence sensitivity to abortion was high before mid-flowering, whereas it was insignificant thereafter, as no inflorescence abortion was detected below the T0 mid-flowering limit. Grapevine berry abscission was also shown to occur over a limited 2-week period after flowering (Bessis and Fournioux, 1992). When comparing the spatial patterns of inflorescence abscission mediated by elevated temperatures on high- and low-initial-vigor plants, two different types of abortion were identified (Figure 2A). For low-vigor plants, an early abortion, starting right after the onset of temperature treatments, followed by a recovery period with a zone without abortions, was observed. In contrast, high-vigor plants displayed a late abortion profile, which is characterized by a period without abortion at the beginning of the temperature treatments, followed by a period of abortion until the end of the experiment.

Based on the internode dry mass and NSC concentrations at harvest (Figures 5B, 6B), the carbon storage at Tf was greater for the high-vigor plants than for the low-vigor plants, regardless of the temperature treatment. However, elevated temperatures massively altered reserve storage in internodes on those high-vigor plants. Because abortion occurred later in development, we proposed the hypothesis that it could be a result of the onset of ripening (*véraison*) at the lower rank (Figure 3). In fact, for both thermal treatments, all the aborted inflorescences were located in the sensitive zone right after the onset of *véraison*. *Véraison* is known to drive a massive

demand for carbohydrates (Pallas et al., 2008; Dai et al., 2009). In addition, several interplaying hormones are involved in grapevine fruit development, either promoting (e.g., abscisic acid, ethylene) or delaying (e.g., auxin) ripening-associated processes (Kuhn et al., 2013). Chervin et al. (2004) reported a peak of ethylene production in berries just before *véraison*. Yet, ethylene and its balance with the above-mentioned hormones are assumed to interact with carbohydrates to induce fruitlet abscission (Sawicki et al., 2015). These elements clearly support the triggering effect of the onset of ripening of the oldest clusters on the activation of abortion in young inflorescences at elevated temperatures.

Remarkably, in spite of the lower carbon storage at Tf for low-vigor plants than for high-vigor plants, temperature had no effect on the final profiles of internode biomass and NSC concentrations, thus suggesting similar carbon pools. However, these profiles for low-vigor plants were performed at a period during which no inflorescence abortion was observed. As *véraison* stage was not reached for low-vigor plants, spatial abortion profiles were not triggered by *véraison*, as in the case of high-vigor plants, and this could explain why the second abortion phase was not observed. As NSC evaluation was performed at a time of no abortion, we cannot conclude about a possible link to carbon status. However, we propose the hypothesis that the high-abortion phase seen early after the passage to higher temperatures was related to a poor plant carbon status at T0, further worsened by elevated temperatures (or improved by low temperatures). Indeed, a low temperature favored a faster recovery of these plants that rapidly entered into a situation of low abortion than in plants that were exposed to elevated temperatures. It is noteworthy that all plants recovered from this situation and showed a long period without abortion later in development, suggesting these plants experienced a global improvement of their carbon status that was more or less delayed because of the temperature treatments. A whole-plant carbon balance, from photosynthesis, respiration, and growth response to elevated temperatures, including the root systems, would permit a better evaluation of the link between this balance and high temperature-induced inflorescence abortion.

Different insights from conducting experiments with high/low initial plant vigor

Thanks to gibberellic acid sensitivity, normal grapevines delay the onset of reproductive development for several (3–5) years. By contrast, *Microvine* is a mutant that lacks the juvenile phase. It is, therefore, conceivable that during the early phases of growth after budbreak, the plant initiates reproductive organs despite being in a difficult situation in terms of reserves.

High-vigor plants were characterized both by thicker shoots before the temperature treatments (+50% compared with low-vigor plants) and by more advanced development than low-vigor plants (55 *vs.* 33 phytomers for high- and low-vigor plants, respectively). The shoot diameter or weight is generally associated with carbohydrate reserve capacity (Rives, 2000; Eltom et al., 2013; Martínez-Lüscher and Kurtural, 2021). The trunk and shoot reserves are important in

grapevine, as they represent about 30% of the total carbon pool (Holzapfel et al., 2010). The absolute concentrations in internode NSC at Tf were comparable to those found normally in grapevine (i.e., 3%–10%) at least during phases of growth (Zapata et al., 2004b; Grechi et al., 2007; Holzapfel et al., 2010). However, for low-vigor plants, the NSC concentrations at Tf were much lower than the ones observed for high-vigor plants in cool temperatures, both in leaves and internodes, suggesting that these plants were suffering from carbon starvation.

The low-vigor plants bring some supplemental, valuable information about grapevine adaptation to abiotic constraints. Indeed, the absence of late abortion for these plants, despite a low NSC, suggests that abortion is not strictly related to sugar content. We thus propose the hypothesis that abortion would not be linked to the carbon status *per se* but rather to the variation of the carbon pool following changes in the source–sink balance. More generally, in indeterminate plants, such as *Microvine*, and independently of temperature treatments, these abortion patterns could be seen as waves. The intense abortion period during the carbon limitation period is followed by a recovery period when the carbon balance becomes more favorable, partly because of abortion, which positively impacts the source-to-sink ratio. Such waves have been described in other indeterminate plants (Wubs et al., 2009). This hypothesis fits with the view that plants are able to sense unbalances in their source-to-sink ratios, such as those induced by various temperatures or day lengths, and implement some physiological strategies, such as the adjustment of their sugar utilization rate (Gibon et al., 2004).

Ultimately, although *Microvine* displays a specific phenotype due to its dwarf size, continuous flowering, and the abortion of inflorescences instead of flowers and fruitlets for grapevine, we believe that the present study provides new insights to better understand and anticipate the impacts of global warming on grapevine functioning. Furthermore, the comparable development of leaf and individual fruit, together with the similar leaf carbon assimilation and sugar storage in fruit and perennial parts in *Microvine*, compared with grapevine (Torregrosa et al., 2017; Torregrosa et al., 2019), make it possible to transfer some of the results obtained in this study to grapevine. As mentioned above, this study showed the importance of considering the pool of sugar to improve the accuracy of grapevine phenological models (flowering, onset of ripening). In addition, our results suggest that more than the total NSC pool, which displays relative homeostasis at different temperatures, the sudden variations of this carbon pool deserve specific attention when studying the impacts of abiotic constraints on grapevine fruitlet abscission. This would be especially important when considering young, productive plants or plants with low vigor and a potential low reserve pool in vineyard conditions (Martínez-Lüscher and Kurtural, 2021).

To conclude, in grapevine elevated temperatures or a low-plant-carbon status generally result in a large reduction in the number of fruits per plant due to lower bud fruitfulness (number of inflorescences per shoot and/or number of flowers per inflorescence), or to lower fruit set. In the present study, we observed high levels of inflorescence abortion in *Microvine* at elevated temperatures, as well as delays in flowering and fruit

ripening stages on the remaining inflorescences. However, the results obtained from the experiments with high- or low-initial-vigor plants suggest that these abortions did not take place either in the same nutritional context or for the same physiological reasons. The high-vigor situation can be easily transposed to a normal grapevine with high vigor and high levels of reserves. In this context, an interaction between elevated temperature and the onset of carbohydrate demand by *véraison* provoked the abortion of inflorescences. In contrast, low-vigor plants, which can also be observed in the vineyard at an early age or in unbalanced growing conditions, appeared to mimic a grapevine recovering from early carbon starvation after a wave of inflorescence abortion provoked by elevated temperatures. Ultimately, this study revealed intense abortion periods when carbon was limited, followed by a possible recovery period when the carbon balance became more favorable, partly because of abortion, which had positive feedback on the source-to-sink ratio.

Data availability statement

The raw data supporting the conclusions of this article will be made available by the authors, without undue reservation.

Author contributions

NL: Formal Analysis, Methodology, Writing – original draft. LT: Conceptualization, Funding acquisition, Supervision, Writing – original draft. YG: Writing – review and editing, Methodology. MR: Writing – review and editing, Methodology. CR: Writing – review and editing, Conceptualization, Funding acquisition. AA: Conceptualization, Writing – review and editing. OT: Formal Analysis, Writing – review and editing. BM: Conceptualization, Funding acquisition, Supervision, Writing – original draft. AP: Conceptualization, Funding acquisition, Supervision, Writing – original draft.

Funding

Acknowledgments

Conflict of interest

The authors declare that the research was conducted in the absence of any commercial or financial relationships that could be construed as a potential conflict of interest.

The author(s) MR declared that they were an editorial board member of Frontiers, at the time of submission. This had no impact on the peer review process and the final decision.

Publisher's note

All claims expressed in this article are solely those of the authors and do not necessarily represent those of their affiliated organizations, or those of the publisher, the editors and the reviewers. Any product that may be evaluated in this article, or claim that may be made by its manufacturer, is not guaranteed or endorsed by the publisher.

Supplementary material

The Supplementary Material for this article can be found online at: https://www.frontiersin.org/articles/10.3389/fhort.2023.1267429/full#supplementary-material

SUPPLEMENTARY FIGURE 1
Net photosynthesis **(A)** and respiration **(B)** per leaf at different *Microvine* leaf positions along the proleptic axis for the experiments with the high-vigor (experiments 1 and 2) and low-vigor (experiments 3–5) plants. The net photosynthesis and respiration per leaf were determined from the net photosynthesis and respiration per unit of leaf area () and the individual leaf area on the ranks from apex (RFA) 5, 10, and 25 over the period from T0 to Tf. The different letters represent significant differences at a p-value = 0.05. The bars represent standard deviations. Each value is the average of six plants.

References

Adams, S. R., Cockshull, K. E., and Cave, C. R. J. (2001). Effect of temperature on the growth and development of tomato fruits. *Ann. Bot.* 88, 869–877. doi: 10.1006/anbo.2001.1524

Allakhverdiev, S. I., Kreslavski, V. D., Klimov, V. V., Los, D. A., Carpentier, R., and Mohanty, P. (2008). Heat stress: An overview of molecular responses in photosynthesis. *Photosynth. Res.* 98, 541–550. doi: 10.1007/s11120-008-9331-0

Bessis, R., and Fournioux, J. C. (1992). Zone d'abscission et coulure de la vigne. *Vitis* 31, 9–21. doi: 10.5073/vitis.1992.31.9-21

Cardell, M. F., Amengual, A., and Romero, R. (2019). Future effects of climate change on the suitability of wine grape production across Europe. *Reg. Environ. Change* 19, 2299–2310. doi: 10.3390/atmos12040495

Chaïb, J., Torregrosa, L., MacKenzie, D., Corena, P., Bouquet, A., and Thomas, M. R. (2010). The grape microvine - A model system for rapid forward and reverse genetics of grapevines. *Plant J.* 62, 1083–1092. doi: 10.1111/j.1365-313X.2010.04219.x

Chervin, C., El-Kereamy, A., Roustan, J. P., Latché, A., Lamon, J., and Bouzaye, M. (2004). Ethylene seems required for the berry development and ripening in

grape, a non-climacteric fruit. *Plant Sci.* 167, 1301–1305. doi: 10.1016/j.plantsci.2004.06.026

Chmielewski, F. M., and Rötzer, T. (2001). Response of tree phenology to climate change across Europe. *Agric. For. Meteorol.* 108, 101–112. doi: 10.1016/s0168-1923(01)00233-7

Civello, P. M., Martinez, G. A., Chaves, A. R., and Anon, M. C. (1997). Heat treatments delay ripening and postharvest decay of strawberry fruit. *J. Agric. Food Chem.* 45, 4589–4594. doi: 10.1021/jf9700337

Coombe, B. G. (1995). Adoption of a system for identifying grapevine growth stages. *Aust. J. Grape Wine Res.* 1, 100–110. doi: 10.1111/j.1755-0238.1995.tb00086.x

Dai, Z. W., Vivin, P., Robert, T., Milin, S., Li, S. H., and Génard, M. (2009). Model-based analysis of sugar accumulation in response to sourcesink ratio and water supply in grape (Vitis vinifera) berries. *Funct. Plant Biol.* 36, 527–540. doi: 10.1071/FP08284

Dewar, R. C., Medlyn, B. E., and McMurtrie, R. E. (1999). Acclimation of the respiration/photosynthesis ratio to temperature: insights from a model. *Glob. Change Biol.* 5, 612–622. doi: 10.1046/j.1365-2486.1999.00253.x

Drake, J. E., Furze, M. E., Tjoelker, M. G., Carrillo, Y., Barton, C. V. M., and Pendall, E. (2019). Climate warming and tree carbon use efficiency in a whole-tree $^{13}CO_2$ tracer study. *New Phytol.* 222, 1313–1324. doi: 10.1111/nph.15721

Dry, P. R., Longbottom, M. L., McLoughlin, S., Johnson, T. E., and Collins, C. (2010). Classification of reproductive performance of ten winegrape varieties. *Aust. J. Grape Wine Res.* 16, 47–55. doi: 10.1111/j.1755-0238.2009.00085.x

Eltom, M., Trought, M., and Winefield, C. (2013). The effects of cane girdling before budbreak on shoot growth, leaf area and carbohydrate content of Vitis vinifera L. Sauvignon Blanc grapevines. *Funct. Plant Biol.* 40, 749–757. doi: 10.1071/FP12278

Fraga, H., García de Cortázar Atauri, I., Malheiro, A. C., and Santos, J. A. (2016). Modelling climate change impacts on viticultural yield, phenology and stress conditions in Europe. *Glob. Change Biol.* 22, 3774–3788. doi: 10.1111/gcb.13382

Gibon, Y., Bläsing, O. E., Palacios-Rojas, N., Pankovic, D., Hendriks, J. H. M., Fisahn, J., et al. (2004). Adjustment of diurnal starch turnover to short days: Depletion of sugar during the night leads to a temporary inhibition of carbohydrate utilization, accumulation of sugars and post-translational activation of ADP-glucose pyrophosphorylase in the following light period. *Plant J.* 39, 847–862. doi: 10.1111/j.1365-313X.2004.02173.x

Gibon, Y., Pyl, E. T., Sulpice, R., Lunn, J. E., Höhne, M., Günther, M., et al. (2009). Adjustment of growth, starch turnover, protein content and central metabolism to a decrease of the carbon supply when Arabidopsis is grown in very short photoperiods. *Plant Cell Environ.* 32, 859–874. doi: 10.1111/j.1365-3040.2009.01965.x

Grechi, I., Vivin, P., Hilbert, G., Milin, S., Robert, T., and Gaudillère, J. P. (2007). Effect of light and nitrogen supply on internal C:N balance and control of root-to-shoot biomass allocation in grapevine. *Environ. Exp. Bot.* 59, 139–149. doi: 10.1016/j.envexpbot.2005.11.002

Greer, D. H., and Weston, C. (2010). Heat stress affects flowering, berry growth, sugar accumulation and photosynthesis of Vitis vinifera cv. Semillon grapevines grown in a controlled environment. *Funct. Plant Biol.* 37, 206–214. doi: 10.1071/FP09209

Hilty, J., Muller, B., Pantin, F., and Leuzinger., S. (2021). Plant growth: the what, the how, and the why. *New Phytol.* 232, 25–41. doi: 10.1111/nph.17610

Holzapfel, B. P., Smith, J. P., Field, S. K., and Hardie, W. J. (2010). Dynamics of carbohydrate reserves in cultivated grapevines. *Hortic. Rev.* 37, 143–211. doi: 10.1002/9780470543672.ch3

Keeling, P. L., Bacon, P. J., and Holt, D. C. (1993). Elevated temperature reduces starch deposition in wheat endosperm by reducing the activity of soluble starch synthase. *Planta* 191, 342–348. doi: 10.1007/BF00195691

Kliewer, W. M., and Dokoozlian, N. K. (2005). Leaf area/crop weight ratios of grapevines: influence on fruit composition and wine quality. *Am. J. Enol. Vitic.* 56, 170–181. doi: 10.5344/ajev.2005.56.2.170

Kuhn, N., Guan, L., Dai, Z. W., Wu, B. H., Lauvergeat, V., Gomès, E., et al. (2013). Berry ripening: recently heard through the grapevine. *J. Exp. Bot.* 65, 16, 4543–4559. doi: 10.1093/jxb/ert395

Lebon, E., Pellegrino, A., Tardieu, F., and Lecoeur, J. (2004). Shoot development in grapevine (Vitis vinifera) is affected by the modular branching pattern of the stem and intra- and inter-shoot trophic competition. *Ann. Bot.* 93, 263–274. doi: 10.1093/aob/mch038

Lebon, G., Duchêne, E., Brun, O., Magné, C., and Clément, C. (2004). Flower abscission and inflorescence carbohydrates in sensitive and non-sensitive cultivars of grapevine. *Sex Plant Reprod.* 17, 71–79. doi: 10.1007/s00497-004-0217-9

Lebon, G., Wojnarowiez, G., Holzapfel, B., Fontaine, F., Vaillant-Gaveau, N., and Clément, C. (2008). Sugars and flowering in the grapevine (Vitis vinifera L.). *J. Exp. Bot.* 59, 2565–2578. doi: 10.1093/jxb/ern135

Liu, J., Zhang, H., Cheng, Y., Wang, J., Zhao, Y., and Geng, W. (2014). Comparison of ultrastructure, pollen tube growth pattern and starch content in developing and abortive ovaries during the progamic phase in hazel. *Front. Plant Sci.* 5. doi: 10.3389/fpls.2014.00528

Lobell, D. B., Field, C. B., Cahill, K. N., and Bonfils, C. (2006). Impacts of future climate change on California perennial crop yields: Model projections with climate and crop uncertainties. *Agric. For. Meteorol.* 141, 208–218. doi: 10.1016/j.agrformet.2006.10.006

Luchaire, N., Rienth, M., Romieu, C., Nehe, A., Chatbanyong, R., Houel, C., et al. (2017). Microvine: A new model to study grapevine growth and developmental patterns

and their responses to elevated temperature. *Am. J. Enol. Vitic.* 68, 283–292. doi: 10.5344/ajev.2017.16066

Martínez-Lüscher, J., and Kurtural, S. K. (2021). Same season and carry-over effects of source-sink adjustments on grapevine yields and non-structural carbohydrates. *Front. Plant Sci.* 12. doi: 10.3389/fpls.2021.695319

Meicenheimer, R. D. (2014). The plastochron index: Still useful after nearly six decades. *Am. J. Bot.* 101, 1821–1835. doi: 10.3732/ajb.1400305

Moriondo, M., Giannakopoulos, C., and Bindi, M. (2011). Climate change impact assessment: The role of climate extremes in crop yield simulation. *Clim. Change* 104, 679–701. doi: 10.1007/s10584-010-9871-0

Pallas, B., Louarn, G., Christophe, A., Lebon, E., and Lecoeur, J. (2008). Influence of intra-shoot trophic competition on shoot development in two grapevine cultivars (Vitis vinifera). *Physiol. Plant* 134, 49–63. doi: 10.1111/j.1399-3054.2008.01100.x

Parent, B., Turc, O., Gibon, Y., Stitt, M., and Tardieu, F. (2010). Modelling temperature-compensated physiological rates, based on the co-ordination of responses to temperature of developmental processes. *J. Exp. Bot.* 61, 2057–2069. doi: 10.1093/jxb/erq003

Perkins-Kirkpatrick, S. E., and Lewis, S. C. (2020). Increasing trends in regional heatwaves. *Nat. Commun.* 11, 3357. doi: 10.1038/s41467-020-16970-7

Poorter, H., Niinemets, Ü., Poorter, L., Wright, I. J., and Villar, R. (2009). Causes and consequences of variation in leaf mass per area (LMA): A meta-analysis. *New Phytol.* 182, 565–588. doi: 10.1111/j.1469-8137.2009.02830.x

Poorter, H., Niklas, K. J., Reich, P. B., Oleksyn, J., Poot, P., and Mommer, L. (2012). Biomass allocation to leaves, stems and roots: Meta-analyses of interspecific variation and environmental control. *New Phytol.* 193, 30–50. doi: 10.1111/j.1469-8137.2011.03952.x

Prasad, P. V. V., Pisipati, S. R., Ristic, Z., Bukovnik, U., and Fritz, A. K. (2008). Impact of nighttime temperature on physiology and growth of spring wheat. *Crop Sci.* 48, 2372–2380. doi: 10.2135/cropsci2007.12.0717

Rives, M. (2000). Vigour, pruning, cropping in the grapevine (Vitis vinifera L.). I. A literature review. *Agronomie* 20, 79–91. doi: 10.1051/agro:2000109

Rogiers, S. Y., Holzapfel, B. P., and Smith, J. P. (2011). Sugar accumulation in roots of two grape varieties with contrasting response to water stress. *Ann. Appl. Biol.* 159, 399–413. doi: 10.1111/j.1744-7348.2011.00505.x

Rolland, F., Baena-Gonzalez, E., and Sheen, J. (2006). Sugar sensing and signaling in plants: conserved and novel mechanisms. *Annu. Rev. Plant Biol.* 57, 675–709. doi: 10.1146/annurev.arplant.57.032905.105441

Ruan, Y. L., Patrick, J. W., Bouzayen, M., Osorio, S., and Fernie, A. R. (2012). Molecular regulation of seed and fruit set. *Trends Plant Sci.* 17, 656–665. doi: 10.1016/j.tplants.2012.06.005

Sadok, W., and Jagadish, S. V. K. (2020). The hidden costs of nighttime warming on yields. *Trends Plant Sci.* 25, 644–651. doi: 10.1016/j.tplants.2020.02.003

Sadras, V. O., and Moran, M. A. (2013a). Asymmetric warming effect on the yield and source: Sink ratio of field-grown grapevine. *Agric. For. Meteorol.* 173, 116–126. doi: 10.1016/j.agrformet.2012.12.005

Sadras, V. O., and Moran, M. A. (2013b). Nonlinear effects of elevated temperature on grapevine phenology. *Agric. For. Meteorol.* 173, 107–115. doi: 10.1016/j.agrformet.2012.10.003

Sadras, V. O., and Petrie, P. R. (2011). Climate shifts in south-eastern Australia: Early maturity of Chardonnay, Shiraz and Cabernet Sauvignon is associated with early onset rather than faster ripening. *Aust. J. Grape Wine Res.* 17, 199–205. doi: 10.1111/j.1755-0238.2011.00138.x

Sawicki, M., Aït Barka, E., Clément, C., Vaillant-Gaveau, N., and Jacquard, C. (2015). Cross-talk between environmental stresses and plant metabolism during reproductive organ abscission. *J. Exp. Bot.* 66, 1707–1719. doi: 10.1093/jxb/eru533

Sgubin, G., Swingedouw, D., Dayon, G., García, de Cortázar-Atauri, I., Ollat, N., Pagé, C., et al. (2018). The risk of tardive frost damage in French vineyards in a changing climate. *Agric. For. Meteorol.* 250–251, 226–242. doi: 10.1016/j.agrformet.2017.12.253

Shahood, R., Torregrosa, L., Savoi, S., and Romieu, C. (2020). First quantitative assessment of growth, sugar accumulation and malate breakdown in a single ripening berry. *Oeno One* 54, 1077–1092. doi: 10.20870/oeno-one.2020.54.4.3787

Shavrukov, Y. N., Dry, I. B., Thomas, M. R., Dejong, T. M., and Zwieniecki, M. A. (2003). Inflorescence and bunch architecture development in Vitis vinifera L. *Aust. J. Grape Wine Res.* 10, 116–124. doi: 10.1111/j.1755-0238.2004.tb00014.x

Sperling, O., Kamai, T., Tixier, A., Davidson, A., Jarvis-Shean, K., Raveh, E., et al. (2019). Predicting bloom dates by temperature mediated kinetics of carbohydrate metabolism in deciduous trees. *Agric. For. Meteorol.*, 276–277. doi: 10.1016/j.agrformet.2019.107643

Suwa, R., Hakata, H., Hara, H., El-Shemy, H. A., Adu-Gyamfi, J. J., Nguyen, N. T., et al. (2010). High temperature effects on photosynthate partitioning and sugar metabolism during ear expansion in maize (Zea mays L.) genotypes. *Plant Physiol. Biochem.* 48, 124–130. doi: 10.1016/j.plaphy.2009.12.010

Thomas, D. S., Montagu, K. D., and Conroy, J. P. (2007). Temperature effects on wood anatomy, wood density, photosynthesis and biomass partitioning of Eucalyptus grandis seedlings. *Tree Physiol.* 27, 251–260. doi: 10.1093/treephys/27.2.251

Torregrosa, L., Bigard, A., Doligez, A., Lecourieux, D., Rienth, M., Luchaire, N., et al. (2017). Developmental, molecular and genetic studies on grapevine response to

temperature open breeding strategies for adaptation to warming. *Oeno One* 51, 155–165. doi: 10.20870/oeno-one.2017.51.2.1587

Torregrosa, L., Rienth, M., Romieu, C., and Pellegrino, A. (2019). The microvine, a model for studies in grapevine physiology and genetics. *Oeno One* 53, 373–391. doi: 10.20870/oeno-one.2019.53.3.2409

Van Leeuwen, C., Destrac-Irvine, A., Dubernet, M., Duchêne, E., Gowdy, M., Marguerit, E., et al. (2019). An update on the impact of climate change in viticulture and potential adaptations. *Agronomy* 9, 1–20. doi: 10.3390/agronomy9090514

Vasconcelos Ribeiro, R., MaChado, E. C., Espinoza-Núñez, E., Ramos, R. A., São, D. F., and MaChado, P. (2012). Moderate warm temperature improves shoot growth, affects carbohydrate status and stimulates photosynthesis of sweet orange plants. *Braz. J. Plant Physiol.* 24 (1), 37–46. doi: 10.1590/S1677-04202012000100006

Vile, D., Pervent, M., Belluau, M., Vasseur, F., Bresson, J., Muller, B., et al. (2012). Arabidopsis growth under prolonged high temperature and water deficit: Independent or interactive effects? *Plant Cell. Environ.* 35, 702–718. doi: 10.1111/j.1365-3040.2011.02445.x

Wang, J., Duan, B., and Zhang, Y. (2012). Effects of experimental warming on growth, biomass allocation, and needle chemistry of Abies faxoniana in even-aged monospecific stands. *Plant Ecol.* 213, 47–55. doi: 10.1007/s11258-011-0005-1

Way, D. A., and Sage, R. F. (2008). Elevated growth temperatures reduce the carbon gain of black spruce [Picea mariana (Mill.) B.S.P.]. *Glob. Change Biol.* 14, 624–636. doi: 10.1111/j.1365-2486.2007.01513.x

Wheeler, T. R., Craufurd, P. Q., Ellis, R. H., Porter, J. R., and Prasad, P. V. V. (2000). Temperature variability and the yield of annual crops. *Agric. Ecosyst. Environ.* 82, 159–167. doi: 10.1016/S0167-8809(00)00224-3

Wilhelm, W. W., and McMaster, G. S. (1995). Importance of the phyllochron in studying development and growth in grasses. *Crop Sci.* 35, 1–3. doi: 10.2135/cropsci1995.0011183X003500010001x

Wubs, A. M., Ma, Y., Heuvelink, E., and Marcelis, L. F. M. (2009). Genetic differences in fruit-set patterns are determined by differences in fruit sink strength and a source: Sink threshold for fruit set. *Ann. Bot.* 104, 957–964. doi: 10.1093/aob/mcp181

Yaacoubi, A. E., Malagi, G., Oukabli, A., Hafidi, M., and Legave, J. M. (2014). Global warming impact on floral phenology of fruit trees species in Mediterranean region. *Sci. Hortic.* 180, 243–253. doi: 10.1016/j.scienta.2014.10.041

Yamori, W., Hikosaka, K., and Way, D. A. (2014). Temperature response of photosynthesis in C3, C4, and CAM plants: Temperature acclimation and temperature adaptation. *Photosynth. Res.* 119, 101–117. doi: 10.1007/s11120-013-9874-6

Zapata, C., Deléens, E., Chaillou, S., and Magné, C. (2004a). Mobilisation and distribution of starch and total N in two grapevine cultivars differing in their susceptibility to shedding. *Funct. Plant Biol.* 31, 1127–1135. doi: 10.1007/s11120-013-9874-6

Zapata, C., Deléens, E., Chaillou, S., and Magné, C. (2004b). Partitioning and mobilization of starch and N reserves in grapevine (Vitis vinifera L.). *J. Plant Physiol.* 161, 1031–1040. doi: 10.1016/j.jplph.2003.11.009

Zhang, L., Zhu, L., Yu, M., and Zhong, M. (2016). Warming decreases photosynthates and yield of soybean [Glycine max (L.) Merrill] in the North China Plain. *Crop J.* 4, 139–146. doi: 10.1016/j.cj.2015.12.003

Zhao, D., Reddy, K. R., Kakani, V. G., Koti, S., and Gao, W. (2005). Physiological causes of cotton fruit abscission under conditions of high temperature and enhanced ultraviolet-B radiation. *Physiol. Plant* 124, 189–199. doi: 10.1111/j.1399-3054.2005.00491.x